PHYSICAL REVIEW A **71**, 052902 (2005)

Dynamical interaction effects on an electric dipole moving parallel to a flat solid surface

Isidro Villó-Pérez,[1] Isabel Abril,[2] Rafael Garcia-Molina,[3] and Néstor R. Arista[4]
[1]*Departamento de Electrónica, Universidad Politécnica de Cartagena, E-30202 Cartagena, Spain*
[2]*Departament de Física, Universitat d'Alacant, Apartat 99, E-03080 Alacant, Spain*
[3]*Departamento de Física, Universidad de Murcia, Apartado 4021, E-30080 Murcia, Spain*
[4]*División Colisiones Atómicas, Instituto Balseiro and Centro Atómico Bariloche, Comisión Nacional de Energía Atómica, RA-8400 Bariloche, Argentina*
(Received 30 November 2004; published 31 May 2005)

The interaction experienced by a fast electric dipole moving parallel and close to a flat solid surface is studied using the dielectric formalism. Analytical expressions for the force acting on the dipole, for random and for particular orientations, are obtained. Several features related to the dynamical effects on the induced forces are discussed, and numerical values are obtained for the different cases. The calculated energy loss of the electric dipole provides useful estimations which could be of interest for small-angle scattering experiments using polar molecules.

DOI: 10.1103/PhysRevA.71.052902 PACS number(s): 34.50.Bw, 34.50.Dy, 79.20.Rf

I. INTRODUCTION

The interaction of fast atoms and molecules with solid surfaces is a subject of great interest for current studies of many physical and chemical processes occurring when energetic particles impinge on solid materials [1], having direct interest in terms of basic knowledge on particle-matter interaction, as well as for the large number of current applications dealing with such interactions (see for instance Ref. [2] and references cited therein). The dominant interaction mechanisms have been extensively studied by several authors for the case of pointlike charges and atomic ions [3–6]. But the case of polar molecules or even the simplest case of electric dipoles has received quite limited attention.

Recent studies on dipole-solid interactions have considered the case of electric dipoles moving within the bulk of a solid, using both the dielectric formulation [7] and the density functional approach [8]. In addition, a recent study [9] has shown that the interaction of a polar molecule with a surface can be analyzed in a convenient way by considering the interaction of an electric dipole with its induced image, indicating that important self-alignment effects are expected to occur.

Other relevant aspects of dipole-surface interactions, like a detailed study of dynamical effects in the induced forces, and the projectile energy dissipation produced by such forces, have not yet received an adequate theoretical treatment. The case of electric dipoles interacting with a solid surface is a problem of considerable current interest that requires attention since it could yield useful results for the analysis of more complicated projectiles, like polar atoms or molecules. In fact, the study of the interaction of polar molecules with the bulk of a solid target is limited by the low survival probability of such molecules when penetrating a dense medium; in most cases, the molecule will break up or get ionized, and then the dipole term will be overshadowed by the emerging monopole components.

On the other hand, there is a higher chance of molecular survival in experiments of scattering on solid surfaces. Moreover, there is current interest in studies of atomic and molecular processes using scattering techniques [10,11] as well as in transmission experiments using microcapillaries [12]. These types of experiments may provide an adequate setup for future studies with polarized atomic or molecular projectiles.

The purpose of this work is to perform a detailed theoretical analysis of the interaction between a fast electric dipole and a flat solid surface, illustrating with several calculations the effect of the dynamical forces acting during the interaction, which could lead to tilting and deflection effects as well as energy loss of the dipole. We apply these results to estimate the energy losses expected in scattering experiments using polar molecules interacting at grazing incidence with solid surfaces.

The paper is organized as follows. In the next section we introduce the dielectric formulation for the study of dipole-surface interactions and apply it to the case of dipoles with trajectories parallel to the surface; we derive closed expressions for the longitudinal and transverse forces acting on the dipole for a general as well as for particular orientations of the dipole axis with respect to its velocity. In Sec. III we present and discuss the results of the calculations for different cases, and we provide values of the expected energy losses in grazing-incidence experiments. Finally, in Sec. IV we summarize the main conclusions of this work. Atomic units (a.u.) will be used throughout this work, except where otherwise stated.

II. FORMULATION OF THE DIPOLE-SURFACE INTERACTION

Let us consider a solid surface lying in the xy plane, at $z=0$, separating a medium located at $z\leqslant 0$ from the vacuum at $z>0$; a particle (named 1) with charge Q_1 is moving through the vacuum along the x direction with velocity $\vec{v}$ parallel to and at a fixed distance z_0 from the surface.

The dielectric formulation for the interaction of fast charged particles with solid surfaces is based in a linear response of the target to the perturbation induced by the pro-

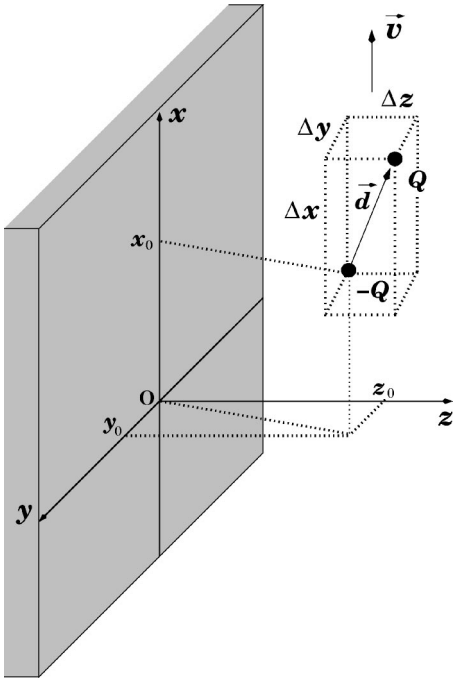

FIG. 1. An electric dipole with dipole moment $\vec{p}=Q\vec{d}$ and velocity $\vec{v}$ is moving along the x direction at a distance z_0 from a plane surface located at $z=0$. The origin of coordinates is taken at the point O, which moves along the surface isotachically with the dipole.

jectile and has been described elsewhere (see, for instance, [13,14] and references contained therein). Within this scheme the induced potential at the coordinates $\vec{r}=(x,y,z)=(\vec{\rho},z)$, due to the charge Q_1 at the position $\vec{r}_1=(x_1,y_1,z_1)=(\vec{\rho}_1,z_1)$, may be written as

$$\Phi_{\mathrm{ind}}^{(1)}(\vec{\rho},z)=-\frac{Q_1}{2\pi}\int_{-\infty}^{+\infty}\frac{d^2k_\rho}{k_\rho}e^{i\vec{k}_\rho\cdot(\vec{\rho}-\vec{\rho}_1)}e^{-k_\rho(z+z_1)}\,\xi(\omega)\big|_{\omega=k_xv}, \tag{1}$$

where $\vec{k}_\rho=(k_x,k_y)$ represents a bidimensional wave vector parallel to the solid surface, and $\omega=\vec{k}\cdot\vec{v}=k_xv$. The surface response function $\xi(\omega)$ is

$$\xi(\omega)=\frac{\epsilon(\omega)-1}{\epsilon(\omega)+1}, \tag{2}$$

where $\epsilon(\omega)$ is the dielectric function of the solid, which depends on the frequency ω corresponding to the electronic excitations that it can sustain.

In order to model the interaction between a fast dipole and a solid surface we consider two charges, of magnitudes $Q_1=-Q$ and $Q_2=Q$, respectively, moving both with the same velocity $\vec{v}$ in the x direction parallel to the surface. This configuration is shown schematically in Fig. 1, the positions of the charges that form the dipole being $\vec{r}_1=(\vec{\rho}_1,z_1)=(x_0,y_0,z_0)$ and $\vec{r}_2=(\vec{\rho}_2,z_2)=(x_0+\Delta x,y_0+\Delta y,z_0+\Delta z)$. Thus, the dipole vector is $\vec{d}=(\Delta x,\Delta y,\Delta z)$ and the dipole moment is $\vec{p}=Q\vec{d}=(Q\Delta x,Q\Delta y,Q\Delta z)$.

The electric field induced at the position $(\vec{\rho},z)$ by the charge Q_i located at $(\vec{\rho}_i,z_i)$ is $\vec{E}_{\mathrm{ind}}^{(i)}=-\vec{\nabla}\Phi_{\mathrm{ind}}^{(i)}$, and can be obtained from Eq. (1),

$$\vec{E}_{\mathrm{ind}}^{(i)}(\vec{\rho},z)=\frac{Q_i}{2\pi}\int_{-\infty}^{+\infty}\frac{d^2k_\rho}{k_\rho}\begin{pmatrix}ik_x\\ik_y\\-k_\rho\end{pmatrix}e^{i\vec{k}_\rho\cdot(\vec{\rho}-\vec{\rho}_i)}e^{-k_\rho(z+z_i)}\,\xi(\omega)\big|_{\omega=k_xv}. \tag{3}$$

The force $\vec{F}_{ij}$ acting on the charge Q_j situated at $(\vec{\rho}_j,z_j)$ due to Q_i is $\vec{F}_{ij}(\vec{\rho}_j,z_j)=Q_j\vec{E}_{\mathrm{ind}}^{(i)}(\vec{\rho}_j,z_j)$, which yields the following expression:

$$\vec{F}_{ij}=\frac{Q_jQ_i}{2\pi}\int_{-\infty}^{+\infty}\frac{d^2k_\rho}{k_\rho}\begin{pmatrix}ik_x\\ik_y\\-k_\rho\end{pmatrix}e^{i\vec{k}_\rho\cdot(\vec{\rho}_j-\vec{\rho}_i)}e^{-k_\rho(z_j+z_i)}\,\xi(\omega)\big|_{\omega=k_xv}. \tag{4}$$

The total force acting on the charge Q_j will be $\vec{F}_{ij}+\vec{F}_{jj}$, where $\vec{F}_{jj}$ is the self-force induced by the charge Q_j on itself. Then, the total force acting on the dipole will be

$$\vec{F}=\sum_{j=1}^{2}\sum_{i=1}^{2}\vec{F}_{ij}. \tag{5}$$

The components of this total force have the following expression:

$$\begin{pmatrix}F_x\\F_y\\F_z\end{pmatrix}=-\frac{Q^2}{2\pi}\int_{-\infty}^{+\infty}\frac{d^2k_\rho}{k_\rho}\begin{pmatrix}ik_x\\ik_y\\-k_\rho\end{pmatrix}g(\vec{k}_\rho)\,\xi(\omega)\big|_{\omega=k_xv}, \tag{6}$$

where

$$g(\vec{k}_\rho)=[2e^{-k_\rho\Delta z}\cos(\vec{k}_\rho\cdot\Delta\vec{\rho})-e^{-2k_\rho\Delta z}-1]e^{-2z_0k_\rho}, \tag{7}$$

with $\Delta\vec{\rho}=\vec{\rho}_2-\vec{\rho}_1=(\Delta x,\Delta y)$.

In order to obtain the dipolar limit, we make a Taylor expansion in Eq. (7) retaining terms up to second order, which gives

$$g(\vec{k}_\rho)\simeq-[(\vec{k}_\rho\cdot\Delta\vec{\rho})^2+(k_\rho\Delta z)^2]e^{-2z_0k_\rho}, \tag{8}$$

which is valid for $|\vec{d}|\ll z_0$.

Inserting Eq. (8) into Eq. (6) we obtain the dipolar approximation for the total force acting on the dipole,

$$\begin{pmatrix}F_x\\F_y\\F_z\end{pmatrix}=\frac{1}{2\pi}\int_{-\infty}^{+\infty}\frac{d^2k_\rho}{k_\rho}\begin{pmatrix}ik_x\\ik_y\\-k_\rho\end{pmatrix}[(\vec{k}_\rho\cdot\vec{p})^2+(k_\rho p_z)^2]e^{-2z_0k_\rho}\,\xi(\omega)\big|_{\omega=k_xv}. \tag{9}$$

Now we separate the surface response function $\xi(\omega)$ into a real part ξ' and an imaginary part ξ'',

$$\xi(\omega)=\xi'(\omega)+i\xi''(\omega). \tag{10}$$

Taking into account the even or odd character in ω of the functions appearing in Eq. (9), the components of the total force acting on the dipole can be rewritten as

$$\begin{pmatrix} F_x \\ F_y \\ F_z \end{pmatrix} = -\frac{1}{2\pi}\int_{-\infty}^{+\infty} \frac{d^2k_\rho}{k_\rho} \begin{pmatrix} \xi''(\omega)k_x \\ \xi''(\omega)k_y \\ \xi'(\omega)k_\rho \end{pmatrix} [(\vec{k}_\rho \cdot \vec{p})^2 + (k_\rho p_z)^2]\, e^{-2z_0 k_\rho}\big|_{\omega=k_x v}. \quad (11)$$

Note the dissipative character of the F_x and F_y forces because of their dependence on the imaginary part of the surface response function ξ'', whereas F_z is a conservative force (image force for the dipole) because it is related to the real part of the surface response function ξ'.

After some algebra, Eq. (11) can be conveniently expressed in matrix form as

$$\begin{pmatrix} F_x \\ F_y \\ F_z \end{pmatrix} = -\frac{1}{2\pi}\int_{-\infty}^{+\infty} dk_x \tilde{A} \begin{pmatrix} p_x^2 + p_z^2 \\ p_y^2 + p_z^2 \\ 2p_x p_y \end{pmatrix}, \quad (12)$$

where $\tilde{A}$ is the (3×3) matrix

$$\tilde{A} = \begin{pmatrix} \xi''(\omega)k_x^3 I_{11} & \xi''(\omega)k_x I_{12} & \xi''(\omega)k_x^2 I_{13} \\ \xi''(\omega)k_x^2 I_{21} & \xi''(\omega) I_{22} & \xi''(\omega)k_x I_{23} \\ \xi'(\omega)k_x^2 I_{31} & \xi'(\omega) I_{32} & \xi'(\omega)k_x I_{33} \end{pmatrix}_{\omega=k_x v}, \quad (13)$$

and the elements I_{ij} $(i,j=1,2,3)$ are integrals in the k_y variable, given by

$$(I_{ij}) = \int_{-\infty}^{+\infty} dk_y \begin{pmatrix} \frac{e^{-2z_0 k_\rho}}{k_\rho} & k_y^2 \frac{e^{-2z_0 k_\rho}}{k_\rho} & k_y \frac{e^{-2z_0 k_\rho}}{k_\rho} \\ k_y \frac{e^{-2z_0 k_\rho}}{k_\rho} & k_y^3 \frac{e^{-2z_0 k_\rho}}{k_\rho} & k_y^2 \frac{e^{-2z_0 k_\rho}}{k_\rho} \\ e^{-2z_0 k_\rho} & k_y^2 e^{-2z_0 k_\rho} & k_y e^{-2z_0 k_\rho} \end{pmatrix}. \quad (14)$$

These integrals can be analytically evaluated, obtaining

$$(I_{ij}) = \begin{pmatrix} 2K_0(2z_0|k_x|) & \frac{|k_x|}{z_0}K_1(2z_0|k_x|) & 0 \\ 0 & 0 & \frac{|k_x|}{z_0}K_1(2z_0|k_x|) \\ 2|k_x|K_1(2z_0|k_x|) & \frac{k_x^2}{z_0}K_2(2z_0|k_x|) & 0 \end{pmatrix}, \quad (15)$$

where $K_n(\cdots)$ denotes the modified Bessel function of the second kind and nth order [15].

Inserting in Eq. (13) the elements I_{ij} from Eq. (15) and using $k_x=\omega/v$, the total force acting on the dipole, Eq. (12), is written as

$$\begin{pmatrix} F_x \\ F_y \\ F_z \end{pmatrix} = -\frac{1}{\pi}\int_0^{+\infty} \frac{d\omega}{v}\tilde{A} \begin{pmatrix} p_x^2 + p_z^2 \\ p_y^2 + p_z^2 \\ 2p_x p_y \end{pmatrix}, \quad (16)$$

with

$$\tilde{A} = \left(\frac{\omega}{v}\right)^2 \begin{pmatrix} 2\xi''(\omega)\frac{\omega}{v}K_0\left(2z_0\frac{\omega}{v}\right) & \frac{1}{z_0}\xi''(\omega)K_1\left(2z_0\frac{\omega}{v}\right) & 0 \\ 0 & 0 & \frac{1}{z_0}\xi''(\omega)K_1\left(2z_0\frac{\omega}{v}\right) \\ 2\xi'(\omega)\frac{\omega}{v}K_1\left(2z_0\frac{\omega}{v}\right) & \frac{1}{z_0}\xi'(\omega)K_2\left(2z_0\frac{\omega}{v}\right) & 0 \end{pmatrix}. \quad (17)$$

Equations (16) and (17) describe the force felt by a dipole moving with velocity v at a distance z_0 parallel to a solid surface, for any orientation of the dipole.

In what follows we will analyze the total force acting on the dipole for three particular orientations, defined by the relative orientation between the dipole moment $\vec{p}$ and the coordinate axis: (A) $\vec{p}\|\hat{x}$, i.e., the dipole moment is parallel to its velocity (along the x direction), (B) $\vec{p}\|\hat{y}$, i.e., the dipole moment is perpendicular to its velocity and parallel to the surface, and (C) $\vec{p}\|\hat{z}$, i.e., the dipole moment is perpendicular to both its velocity and the surface.

To describe the dipole orientation we use spherical coordinates θ and ϕ, where θ is the angle between the dipole and the z direction and ϕ is the angle between the x direction and the projection of the dipole into the xy plane. Thus, the Cartesian components of the dipole moment are

$$p_x = p\sin\theta\cos\phi,$$

$$p_y = p\sin\theta\sin\phi,$$

$$p_z = p\cos\theta. \quad (18)$$

In what follows we analyze separately each one of the above-mentioned cases, indicating the values of the angles θ and ϕ specifying the dipole orientation, the dipole moment $\vec{p}$, and the corresponding force derived from Eq. (16).

A. Parallel orientation $\vec{p}\|\hat{x}$

The parameters of the dipole in this case are $\theta=\pi/2$, $\phi=0$, and $\vec{p}=(p,0,0)$; therefore

$$\begin{pmatrix} F_x \\ F_y \\ F_z \end{pmatrix} = -\frac{2p^2}{\pi}\int_0^{+\infty}\frac{d\omega}{v}\left(\frac{\omega}{v}\right)^3\begin{pmatrix} \xi''(\omega)K_0\left(2z_0\frac{\omega}{v}\right) \\ 0 \\ \xi'(\omega)K_1\left(2z_0\frac{\omega}{v}\right)\end{pmatrix}. \tag{19}$$

B. Transverse orientation $\vec{p}\|\hat{y}$

In this case $\theta=\pi/2$, $\phi=\pi/2$, $\vec{p}=(0,p,0)$, and

$$\begin{pmatrix} F_x \\ F_y \\ F_z \end{pmatrix} = -\frac{p^2}{\pi z_0}\int_0^{+\infty}\frac{d\omega}{v}\left(\frac{\omega}{v}\right)^2\begin{pmatrix} \xi''(\omega)K_1\left(2z_0\frac{\omega}{v}\right) \\ 0 \\ \xi'(\omega)K_2\left(2z_0\frac{\omega}{v}\right)\end{pmatrix}. \tag{20}$$

C. Perpendicular orientation $\vec{p}\|\hat{z}$

Here $\theta=0$, $\vec{p}=(0,0,p)$, and

$$\begin{pmatrix} F_x \\ F_y \\ F_z \end{pmatrix} = -\frac{p^2}{\pi}\int_0^{+\infty}\frac{d\omega}{v}\left(\frac{\omega}{v}\right)^2 \times\begin{pmatrix} 2\xi''(\omega)\frac{\omega}{v}K_0\left(2z_0\frac{\omega}{v}\right)+\frac{1}{z_0}\xi''(\omega)K_1\left(2z_0\frac{\omega}{v}\right) \\ 0 \\ 2\xi'(\omega)\frac{\omega}{v}K_1\left(2z_0\frac{\omega}{v}\right)+\frac{1}{z_0}\xi'(\omega)K_2\left(2z_0\frac{\omega}{v}\right)\end{pmatrix}. \tag{21}$$

We can see that the force in case C is related to the forces in cases A and B through

$$\begin{pmatrix} F_x \\ F_y \\ F_z \end{pmatrix}_{\text{case C}} = \begin{pmatrix} F_x \\ F_y \\ F_z \end{pmatrix}_{\text{case A}} + \begin{pmatrix} F_x \\ F_y \\ F_z \end{pmatrix}_{\text{case B}}. \tag{22}$$

D. Angular average

The case of random orientation of the dipole is of much interest in connection with possible experiments using beams of randomly oriented molecules. For this situation, we shall consider the angular average of Eq. (16), namely

$$\langle\vec{F}\rangle = -\frac{1}{\pi}\int_0^{+\infty}\frac{d\omega}{v}\tilde{A}\begin{pmatrix}\langle p_x^2+p_z^2\rangle \\ \langle p_y^2+p_z^2\rangle \\ \langle 2p_xp_y\rangle\end{pmatrix}, \tag{23}$$

where $\langle\cdots\rangle$ denotes the average over the angular variables.

Using Eq. (18) to calculate the angular integrations in the previous equation we obtain

$$\begin{pmatrix}\langle p_x^2+p_z^2\rangle \\ \langle p_y^2+p_z^2\rangle \\ \langle 2p_xp_y\rangle\end{pmatrix} = \frac{2p^2}{3}\begin{pmatrix}1\\1\\0\end{pmatrix}. \tag{24}$$

Inserting Eq. (24) into Eq. (23) and using Eq. (17), we obtain the following expression for the angular average of the force acting on the dipole:

$$\langle\vec{F}\rangle = -\frac{2p^2}{3\pi}\int_0^{+\infty}\frac{d\omega}{v}\left(\frac{\omega}{v}\right)^2 \times\begin{pmatrix} 2\xi''(\omega)\frac{\omega}{v}K_0\left(2z_0\frac{\omega}{v}\right)+\frac{1}{z_0}\xi''(\omega)K_1\left(2z_0\frac{\omega}{v}\right) \\ 0 \\ 2\xi'(\omega)\frac{\omega}{v}K_1\left(2z_0\frac{\omega}{v}\right)+\frac{1}{z_0}\xi'(\omega)K_2\left(2z_0\frac{\omega}{v}\right)\end{pmatrix}. \tag{25}$$

This result shows a simple relation with case C (perpendicular orientation) given by Eq. (21). Explicitly,

$$\langle\vec{F}\rangle = \frac{2}{3}\vec{F}_{\text{case C}}. \tag{26}$$

An alternative and also useful expression is

$$\langle\vec{F}\rangle = \frac{p^2}{3\pi}\int d^2k_\rho(i\vec{k_\rho},-k_\rho)k_\rho e^{-2k_\rho z_0}\left[\frac{\varepsilon(\omega)-1}{\varepsilon(\omega)+1}\right]. \tag{27}$$

In the next section we will evaluate numerically these integrals for metal surfaces, represented by the simple Drude model

$$\epsilon(\omega) = 1-\frac{\omega_p^2}{\omega(\omega+i\gamma)}, \tag{28}$$

where ω_p and γ are the plasmon frequency and the damping rate characterizing each metal.

III. CALCULATIONS

A. Induced dipole forces

In what follows we apply the previous formulation to study the interaction of electric dipoles moving parallel to a solid surface at a fixed distance, for several relative orientations which are worth discussing. We will consider the following metallic solids: Al, Cu, Ag, and Au, which are characterized by the parameters ω_p and γ; for brevity, we will use the surface-plasmon frequency $\omega_s=\omega_p/\sqrt{2}$. The characteristic values of the metals to be discussed in this work appear in Table I. In all the cases that follow we consider a dipole with $p=3$ a.u., which is a typical value for permanent dipole moments of polar molecules, as can be seen from the data collected in Table II.

TABLE I. Values of the parameters characterizing the surface response of the metals discussed in the text.

Metal	ω_s (a.u.)	γ (a.u.)
Al	0.40	0.037
Cu	0.75	1.2
Ag	1.30	2.8
Au	1.41	2.5

TABLE II. Permanent dipole moments of some molecules.

Molecule	p (a.u.)
H_2O	0.73
LiH	2.29
LiF	2.63
KCl	3.12
NaCl	3.31
KF	3.35
CsCl	3.89

Let us discuss first the case of an aluminum surface, because this target is very well described (better than Cu, Au, or Ag) by a single plasma resonance, i.e., it behaves as a typical Drude model.

In Figs. 2 and 3 we show the velocity dependence of the force experienced by a dipole moving parallel (at a fixed distance $z_0=5$ a.u.) to an aluminum surface. The two panels in Fig. 2 depict the behavior of the stopping and the lateral forces (F_x and F_z, respectively; F_y being zero) acting on the dipole for the three cases A, B, and C, discussed in the previous section. Figure 3 shows the behavior of the force components (F_x,F_y,F_z) acting on the dipole when it lies in the xy plane with $\theta=\pi/2$ and $\phi=\pi/4$; in this case $F_y\neq 0$. It is worth noticing that Figs. 2 and 3 show that $F_x<0$ in all the cases, which means a true stopping force, i.e., opposite to the dipole velocity. However F_z has a more complicated behavior; although in most cases F_z is negative (i.e., there is an attractive force toward the surface, which can be considered the "normal" behavior), when the dipole is parallel to the velocity (case A), F_z becomes positive (i.e., the dipole is repelled from the surface) for $v\gtrsim 1$ a.u., as clearly seen in Fig. 2(b).

Figure 4 shows the behavior of the forces F_x and F_z acting on the dipole, as a function of its velocity v, for several distances between the dipole and the surface, $z_0=4$, 5, and 6 a.u. We only consider the case A, where the dipole moment $\vec{p}$ is parallel to its velocity ($\vec{p}\|\hat{x}$).

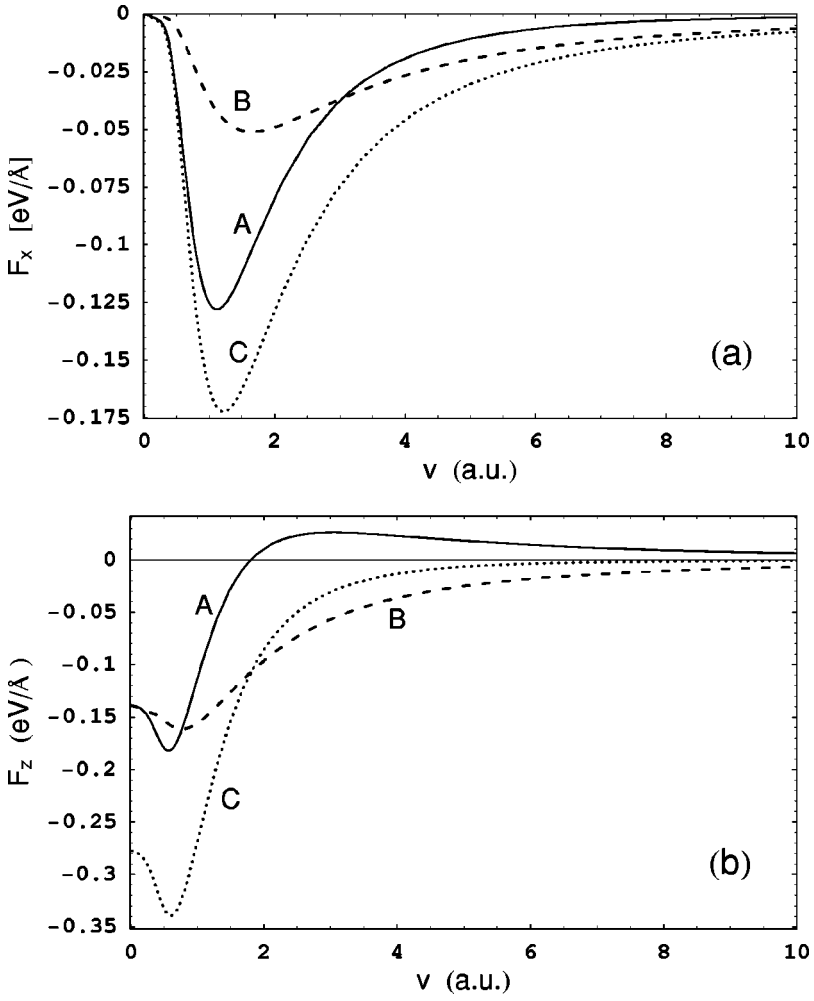

FIG. 2. (a) Stopping force F_x and (b) lateral force F_z as a function of the dipole velocity v, for the cases A, B, and C described in the text, with $z_0=5$ a.u. and $p=3$ a.u. The solid surface is Al. For these three cases $F_y=0$.

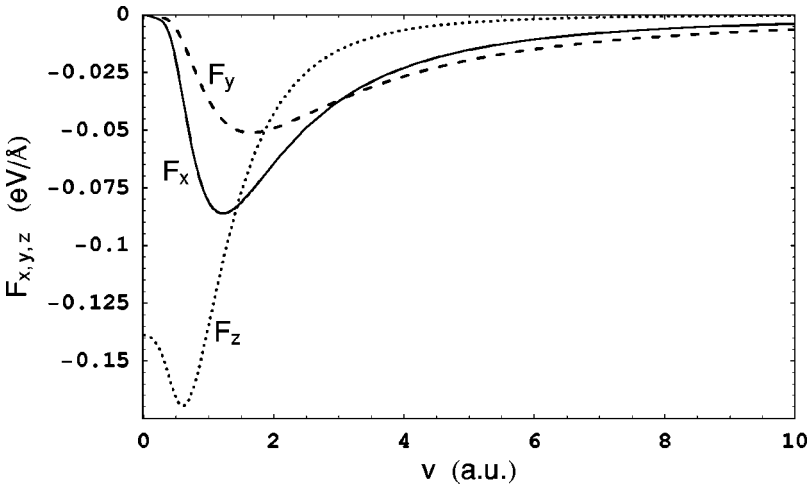

FIG. 3. (F_x,F_y,F_z) components of the force as function of the dipole velocity v, when the dipole is in the plane xy with $\theta=\pi/2$ and $\phi=\pi/4$. The distance is $z_0=5$ a.u. and the dipole moment is $p=3$ a.u. The solid surface is Al. Unlike Fig. 2, now $F_y\neq 0$.

Figure 5 shows (a) the stopping force F_x, and (b) the attraction force F_z, as a function of the velocity v, for the case A, and for different solid surfaces (Al, Cu, Ag, and Au). The distance is $z_0=5$ a.u.. The magnitudes and shapes of the curves that represent these forces are related to the different dielectric properties of each media (see for instance Ref. [14]. These results are analyzed in the following.

The forces F_x and F_y have an intrinsic dynamical character (related to the dynamical response of the medium), hence they drop to zero in the static situation ($v=0$), as can be seen in Figs. 2(a), 3, 4(a), and 5(a). These forces are due to the delay in the response of the surface, which gives rise to a lag of the induced charge in the material (the dynamical "image charge") relative to the instantaneous position of the dipole. On the other hand, F_z has a well-defined static limit [see Figs. 2(b), 3, 4(b), and 5(b)], which may be deduced from the classical interaction energy $U(r)$ between two dipoles $\vec{p}$ and $\vec{p}'$ separated by a distance r,

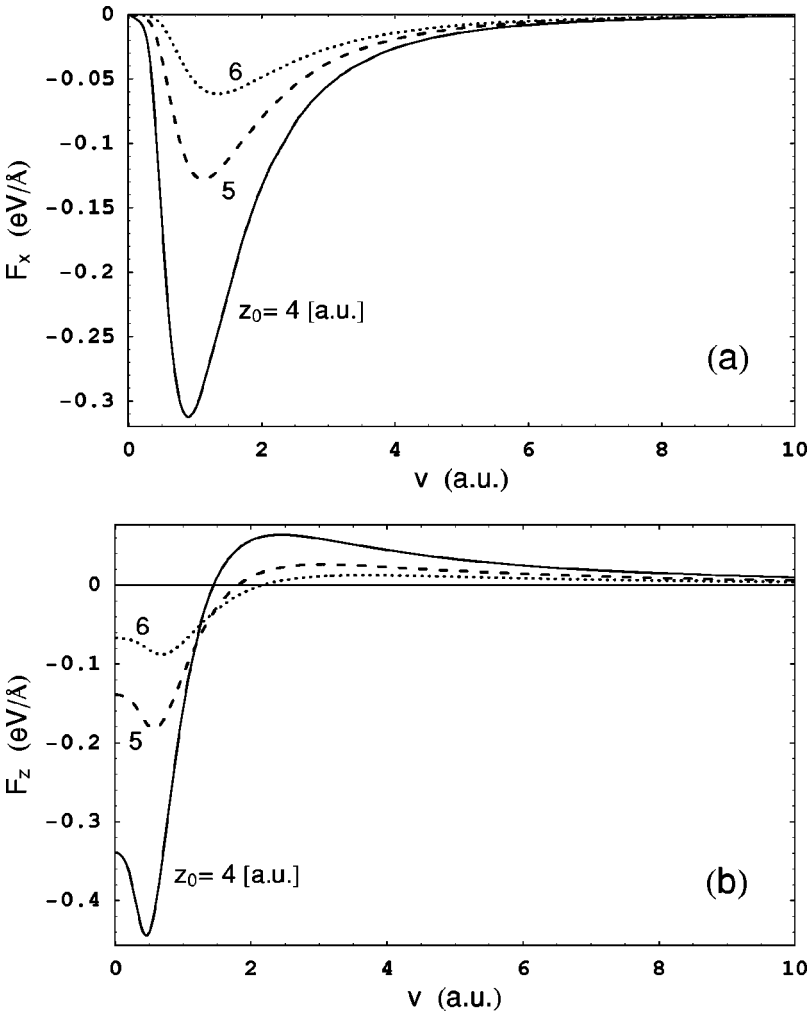

FIG. 4. (a) Stopping force F_x and (b) attractive force F_z as a function of the dipole velocity v, for the case A (parallel dipole orientation) with $p=3$ a.u. and $z_0=4$, 5, and 6 a.u. The solid surface is Al.

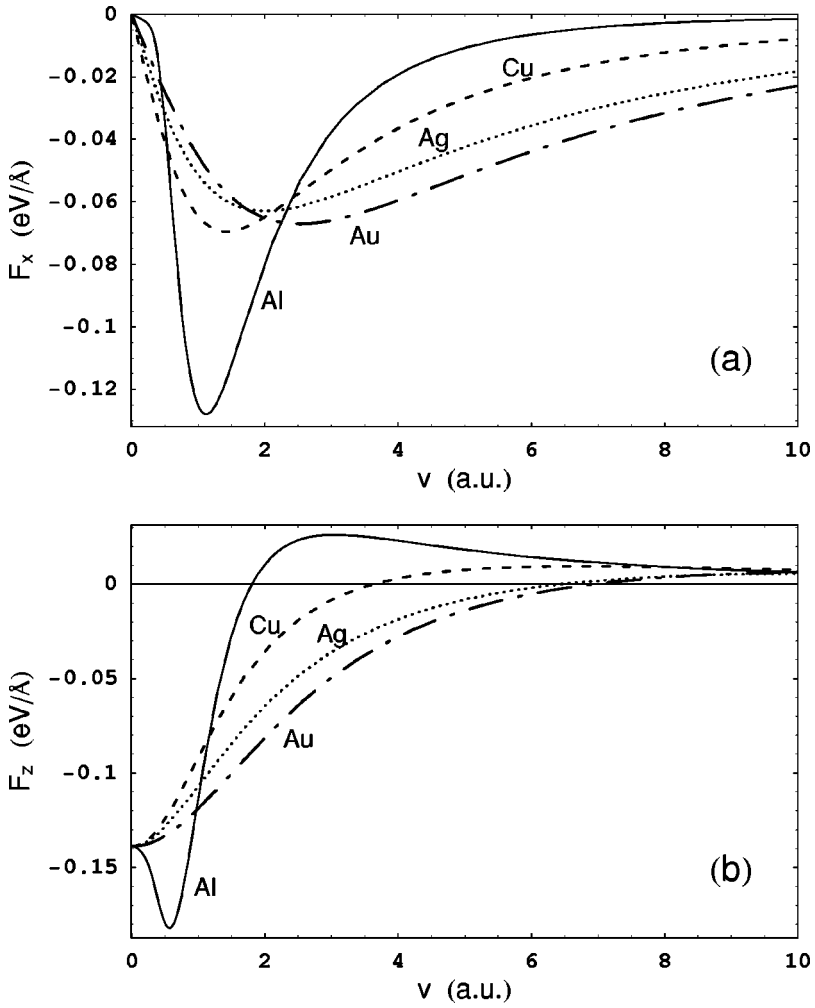

FIG. 5. (a) Stopping force F_x and (b) attractive force F_z as a function of the dipole velocity v, for the case A (parallel dipole orientation) and for different solid surfaces: Al, Cu, Ag, and Au. The distance is $z_0=5$ a.u. and the dipole moment is $p=3$ a.u.

$$U(r)=[\vec{p}\cdot\vec{p}'-3(\vec{p}\cdot\hat{r})(\vec{p}'\cdot\hat{r})]\frac{1}{r^3}, \tag{29}$$

which corresponds to a dipole-dipole type interaction, between the real dipole $\vec{p}$ and a fictitious "image dipole" $\vec{p}'=-\vec{p}$ located at the position $z=-z_0$ (the mirror image). This limit also explains the identical static values for cases A and B observed in Fig. 2(b), which is independent of the surface nature [see Fig. 5(b)], and the greater values (in magnitude) obtained for case C. In fact, calculating the force $\vec{F}=-\vec{\nabla}U(r)$ for parallel dipole-surface orientation (static cases A and B), we obtain $F_z^{\parallel}=-3p^2/(2z_0)^4$, whereas for the perpendicular orientation (case C), we get $F_z^{\perp}=-6p^2/(2z_0)^4$. These values exactly agree with the limits found in Figs. 2–5 for the force F_z when $v\to 0$, and also explain the identical values obtained for the four metals in Fig. 5(b).

An additional feature of interest here is the presence of a dip in the F_z values when $v<1$ a.u. for narrow-resonance materials like Al. It may be noted that the same effect appears in the simplest case of a pointlike charge moving parallel to a solid surface [14]. But this effect disappears for materials with wider plasma resonances (like Cu, Ag, and Au) as may be seen in Fig. 5(b) and has also been discussed in Ref. [14].

These different behaviors of F_x, F_y, and F_z can be understood if we have in mind their origin, Eq. (11), which shows that F_x and F_y are related to the dissipative part of the surface response function, $\xi''(\omega)$, whereas F_z is related to the conservative part, $\xi'(\omega)$.

Finally in Fig. 6 we have studied the angular dependence of the forces acting on the dipole according to Eqs. (16) and (18). The dependence of the intensity of the forces with (θ,ϕ) can be conveniently shown by means of a polar graph, as illustrated in Fig. 6(a). In Fig. 6(b) we show the stopping force $|F_x|$ and we observe that it has a maximum when the dipole is oriented along the z axis (perpendicular to the surface, case C, $\theta=0$), and has a minimum when the dipole is oriented along the y axis (parallel to the surface but perpendicular to its velocity, case B, $\theta=\pi/2$ and $\phi=\pi/2$). The lateral force $|F_y|$ is depicted in Fig. 6(c), where we observe that if the dipole lies in the xz or in the yz plane the force $|F_y|$ is always null, and grows when separating from these planes. In particular, the highest values are obtained when the dipole is on the xy plane, with $\phi=\pi/4$, $3\pi/4$, $5\pi/4$, or $7\pi/4$. Finally, Fig. 6(d) shows the values of the perpendicular force $|F_z|$, which represents the attraction toward the surface [note that $F_z<0$ in this case, Fig. 5(b)]. We find that $|F_z|$ has a maximum when the dipole is parallel to the z axis (case C, $\theta=0$) and it has a minimum when the dipole is oriented

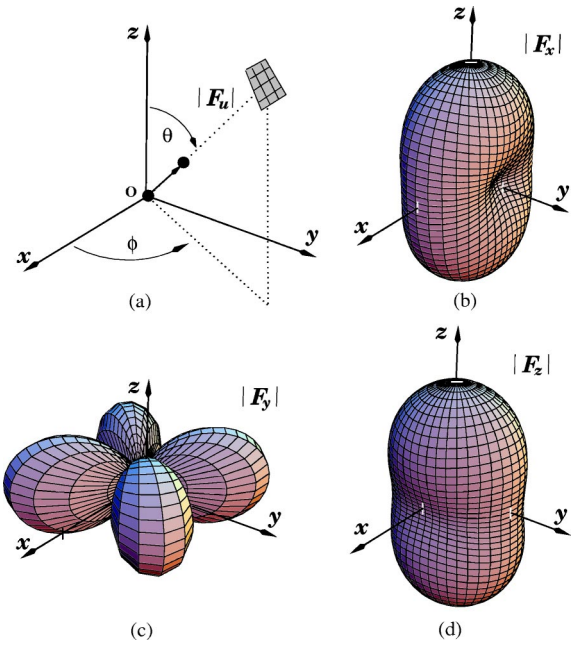

FIG. 6. (Color online) (a) Polar graph for $|F_u|$, $(u=x,y,z)$. For a pair of values (θ,ϕ) the radial distance from the origin O to the surface represented by the mesh is given by $|F_u|$. (b) Stopping force $|F_x|$, (c) $|F_y|$, and (d) $|F_z|$. The solid surface is Au, the velocity is $v=2$ a.u., the distance is $z_0=5$ a.u., and the dipole moment is $p=3$ a.u.

along the x axis (case A, $\theta=\pi/2$ and $\phi=0$). This angular dependence may be qualitatively explained by the simplified picture of the interaction between the real dipole and its image behind the surface.

B. Comparison with pointlike charges

As a final discussion, we will now compare the magnitude of the induced stopping force acting on a dipole with the corresponding one for the reference case of a pointlike charge Q. For illustration purposes we will discuss two orientations of the dipole: parallel (case A) and random. Equations (19) and (25) give the stopping force F_x acting on the dipole in the above-mentioned cases. Although the stopping force acting on a pointlike charge is well known, for clarity in further discussions we show here the explicit forms of these expressions:

$$F_x^{(\text{point charge})} = -\frac{2Q^2}{\pi}\int_0^{+\infty}\frac{d\omega}{v}\frac{\omega}{v}\xi''(\omega)K_0\left(2z_0\frac{\omega}{v}\right), \quad (30)$$

$$F_x^{(\text{case A})} = -\frac{2p^2}{\pi}\int_0^{+\infty}\frac{d\omega}{v}\left(\frac{\omega}{v}\right)^3\xi''(\omega)K_0\left(2z_0\frac{\omega}{v}\right), \quad (31)$$

$$\langle F_x\rangle = -\frac{2p^2}{3\pi}\int_0^{+\infty}\frac{d\omega}{v}\left(\frac{\omega}{v}\right)^2\xi''(\omega)\left[2\frac{\omega}{v}K_0\left(2z_0\frac{\omega}{v}\right) + \frac{1}{z_0}K_1\left(2z_0\frac{\omega}{v}\right)\right]. \quad (32)$$

These stopping forces are shown in Fig. 7 for aluminum and gold surfaces, as a function of the projectile velocity, for a unit charge (proton) $Q=1$ and for a dipole with parallel orientation (case A) assuming a dipole moment $p=3$ a.u. Figure 7(a) depicts the case when the dipole is oriented parallel to the velocity (case A), whereas Fig. 7(b) corresponds to the case of random orientation. We observe from these figures that the maxima of the curves that represent the stopping force corresponding to dipoles are displaced to lower velocities than the analogous curves for pointlike charges, and also that the magnitudes of the stopping force for the former are reduced to $\lesssim 50\%$ the values for the latter.

A useful approximation that serves to illustrate this comparison in simple terms is obtained by using the "plasma-pole approximation" for the imaginary part of the surface-response function, namely,

$$\xi''(\omega) \equiv \text{Im}\left[\frac{\varepsilon(\omega)-1}{\varepsilon(\omega)+1}\right] \cong \frac{\pi}{2}\omega_s\delta(\omega-\omega_s), \quad (33)$$

which corresponds to the condition $\gamma/\omega_s \to 0$, i.e., a narrow plasma resonance. In this case, the stopping forces derived from Eqs. (30)–(32), may be written as follows:

$$F_x^{(\text{point charge})} \cong -(Q^2/z_0^2)f_0(u), \quad (34)$$

$$F_x^{(\text{case A})} \cong -(p^2/z_0^4)f_A(u), \quad (35)$$

$$\langle F_x\rangle \cong -(p^2/z_0^4)f_{\text{av}}(u), \quad (36)$$

where $u=v/(z_0\omega_s)$ and

$$f_0(u) = K_0(2/u)/u^2, \quad (37)$$

$$f_A(u) = K_0(2/u)/u^4, \quad (38)$$

$$f_{\text{av}}(u) = [K_0(2/u) + K_2(2/u)]/3u^4. \quad (39)$$

Note that the identity $K_0(x)+(1/x)K_1(x)=(1/2)[K_0(x)+K_2(x)]$ has been used in order to obtain the last expression. The behavior of these functions is illustrated in Fig. 8. It can be checked that these functions yield a very good approximation to the stopping force values for the case of Al shown previously in Figs. 7(a) and 7(b). Taking into account that the maximum values of these functions are $f_0(u)|_{\max}=0.120$, $f_A(u)|_{\max}=0.184$, and $f_{\text{av}}(u)|_{\max}=0.164$, we obtain the following approximations for the maximum stopping forces corresponding to pointlike charges and to aligned and random dipoles, respectively: $F_x^{(\text{point charge})}|_{\max}\cong 0.120(Q^2/z_0^2)$, $F_x^{(\text{case A})}|_{\max}\cong 0.184(p^2/z_0^4)$, $\langle F_x\rangle|_{\max}\cong 0.164(p^2/z_0^4)$.

The maximum values of these forces are shown in Fig. 9 as a function of the distance z_0, for dipoles with $p=1$ and 3 a.u., as well as for a proton. Note that crossing between the dipole and the pointlike charge maximum forces occurs at $z_0\cong 1$ a.u. for $p=1$ and $z_0\cong 3.5$ a.u. for $p=3$, which approximately determine the shortest distances where the model is applicable. It should be noted that for distances smaller than ~ 2 a.u. one should consider corrections to the dielectric response function arising from spatial dispersion effects [16].

Extrapolating the previous discussions for an electric dipole projectile to the case of polar molecules we conclude

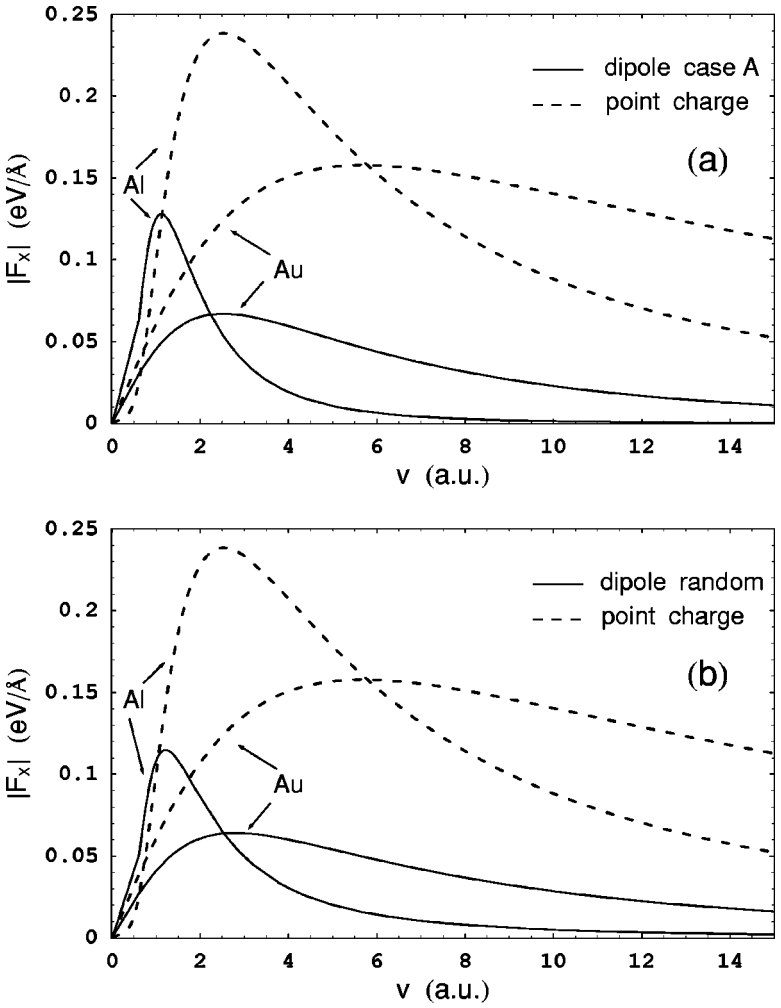

FIG. 7. Stopping force $|F_x|$ for Al and Au, for a unit charge $Q=1$ and for a dipole with dipole moment $p=3$ a.u. (a) Parallel dipole orientation (case A). (b) Random dipole orientation. The distance to the surface is $z_0=5$ a.u.

that the stopping forces acting on the latter are of similar magnitude to those for pointlike charges. Hence, the experimental determination of the energy losses of polar molecules interacting with solid surfaces should be accessible under similar conditions of energy resolution currently used in energy loss experiments with simple atomic ions.

IV. SUMMARY AND CONCLUSIONS

The interaction between a fast electric dipole and a solid surface was studied using the dielectric formulation for the case of fixed dipole-surface distance. General expressions for the longitudinal and transverse forces were derived for arbi-

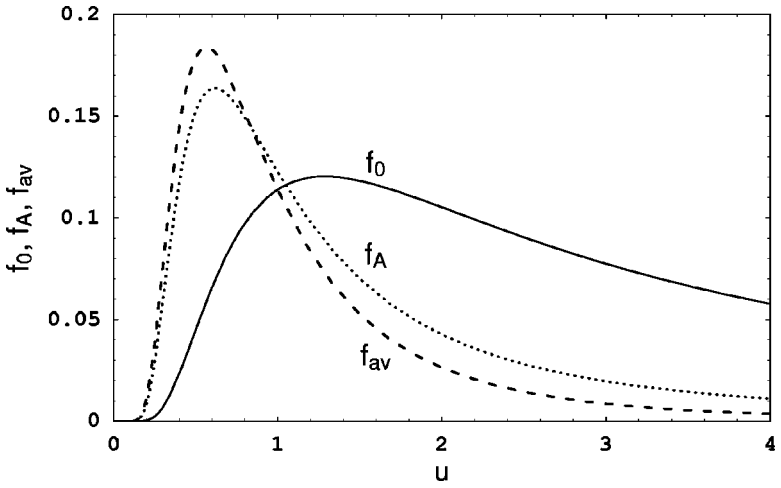

FIG. 8. Functions $f_0(u)$, $f_A(u)$, and $f_{av}(u)$, given by Eqs. (37)–(39), corresponding to the stopping forces for pointlike charges and to aligned (case A) and random dipoles, respectively, in terms of the adimensional scaling variable u, defined as $u=v/(z_0\omega_s)$.

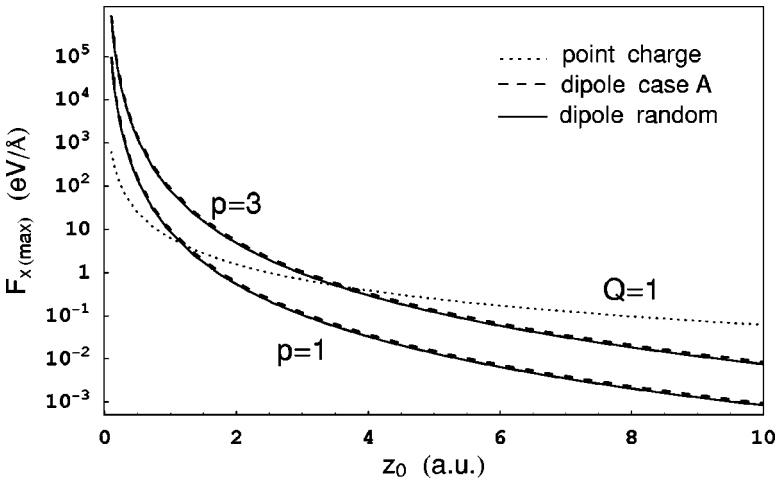

FIG. 9. Maximum values of the stopping forces $F_x^{(\text{point charge})}|_{\max}$, $F_x^{(\text{case A})}|_{\max}$, and $\langle F_x\rangle|_{\max}$ described in the text, for pointlike charges (dotted line), aligned dipoles (dashed lines), and random dipole orientation (solid lines). The calculated values for dipoles correspond to $p=1$ a.u. and 3 a.u., as indicated in the figure.

trary orientation of the dipole, and also particular expressions for the cases of parallel, transverse, and random orientations of the dipole were given. From these results, the stopping force on the dipole was derived for each of these cases.

The behavior of the forces was illustrated through a set of calculations covering all the cases indicated before. The values of the force were computed for different distances to the surface and dipole velocities.

Numerical estimations were obtained for the metallic surfaces Al, Cu, Ag, and Au. The cases of aligned and randomly oriented dipole beams were considered, and the results were compared with similar calculations for the case of a proton, which is a typical pointlike charge. From these estimations we conclude the possibility of measuring the energy losses of polar molecules (the analogous to electric dipoles) by adequate experiments using, for instance, small angles of incidence (similar to experiments regularly done with atomic ions).

In addition, the general formulation and particular results obtained here could be of interest for future studies in the area of atomic collisions with solids and may serve as a guide to design experiments to study various aspects of the interaction between polar molecules and solids surfaces. In a more general context, the present results may be useful also in other fields of research, such as chemical physics and catalysis studies.

ACKNOWLEDGMENTS

This work was supported in part by Fundación Séneca (Project No. PC- MC/7/00063/FS/02), the Spanish Ministerio de Ciencia y Tecnología (Projects No. BFM2003-04457-C02-01 and No. BFM2003-04457-C02-02), and by the Argentinean Agencia Nacional de Promoción Científica y Tecnológica (Project No. PICT-R00122).

[1] *Interaction of Charged Particles with Solids and Surfaces*, edited by A. Gras-Martí, H. M. Urbassek, N. R. Arista, and F. Flores, NATO Advanced Studies Institute, Series B: Physics (Plenum, New York, 1991), Vol. 271.
[2] H. Winter, Phys. Rep. **367**, 387 (2002).
[3] D. Chan and P. Richmond, J. Phys. C **9**, 163 (1976).
[4] T. L. Ferrell, P. M. Echenique, and R. H. Ritchie, Solid State Commun. **32**, 419 (1979).
[5] J. R. Manson and R. H. Ritchie, Phys. Rev. B **29**, 1084 (1984).
[6] R. Garcia-Molina, A. Gras-Martí, A. Howie, and R. H. Ritchie, J. Phys. C **18**, 5335 (1985).
[7] N. R. Arista, Phys. Rev. A **65**, 022902 (2002).
[8] M. Alducin, R. Diez-Muiño, J. I. Juaristi, and P. M. Echenique, Phys. Rev. A **66**, 054901 (2002).
[9] S. K. Sekatskii, Phys. Rev. A **67**, 022901 (2003).
[10] I. Stensgaard, Rep. Prog. Phys. **55**, 989 (1992).
[11] H. Niehus, W. Heiland, and E. Taglauer, Surf. Sci. Rep. **17**, 213 (1993).
[12] Y. Yamazaki, S. Ninomiya, F. Koike, H. Masuda, T. Azuma, K. Komaki, K. Kuroki, and M. Sekiguchi, J. Phys. Soc. Jpn. **65**, 1199 (1996); S. Ninomiya, Y. Yamazaki, F. Koike, H. Masuda, T. Azuma, K. Komaki, K. Kuroki, and M. Sekigu, Phys. Rev. Lett. **78**, 4557 (1997).
[13] P. M. Echenique, R. H. Ritchie, N. Barberán, and J. Inkson, Phys. Rev. B **23**, 6486 (1981).
[14] N. R. Arista, Phys. Rev. A **49**, 1885 (1994).
[15] *Handbook of Mathematical Functions, with Formulas, Graphs, and Mathematical Tables*, edited by M. Abramowitz and I. A. Stegun (Dover, New York, 1972), Chap. 9.
[16] C. Denton, J. L. Gervasoni, R. O. Barrachina, and N. R. Arista, Phys. Rev. A **57**, 4498 (1998).